

Supplementary Materials for
ULK1-mediated metabolic reprogramming regulates Vps34 lipid kinase activity by its lactylation

Mengshu Jia *et al.*

Corresponding author: Xiawei Cheng, chengxw@ecust.edu.cn; Yuzheng Zhao, yuzhengzhao@ecust.edu.cn;
Yi Yang, yiyang@ecust.edu.cn

Sci. Adv. **9**, eadg4993 (2023)
DOI: 10.1126/sciadv.adg4993

This PDF file includes:

Figs. S1 to S7
Table S1

Fig.S1

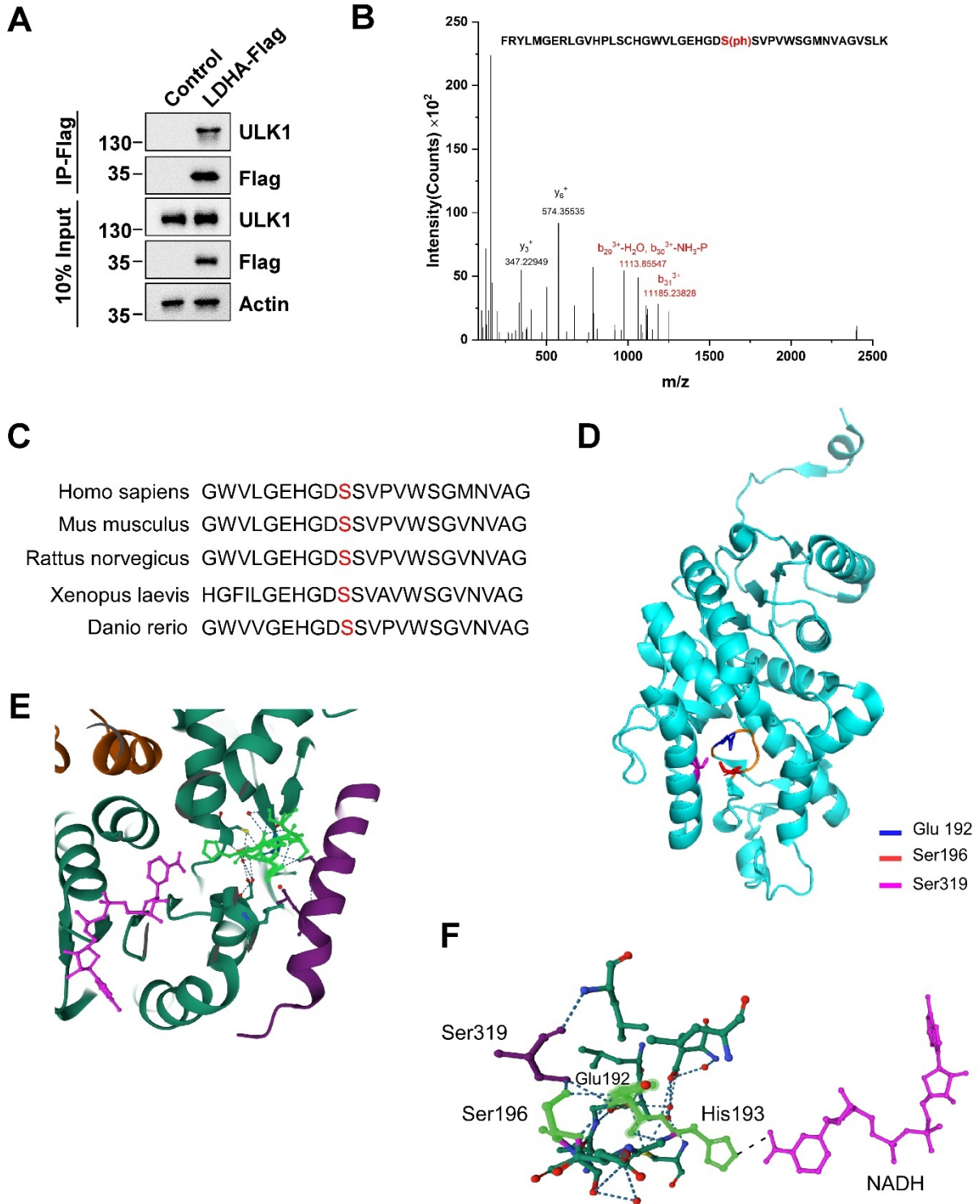


Fig.S1. LDHA is a substrate of ULK1.

(A) Interaction assay of endogenous ULK1 and LDHA. LDHA-Flag was expressed in HEK293T cells. Immunoprecipitation was performed using anti-Flag beads and analyzed by western blot with antibody to ULK1. (B) Identification of LDHA phosphorylation at Serine 196 by mass spectrometry. (C) Alignment of sequences of LDHA from various species. Red indicates the identified phosphorylation site of LDHA. (D) Spatial conformation of LDHA. The region Glycine191–Serine197 in LDHA forms a loop. Images were created using Pymol (<http://www.pymol.org>) and Protein Data Bank (PDB) accession 5ZJD. (E-F) The Serine196 and Glutamate192 in the loop maintain LDHA conformation with Serine 319 by hydrogen bond. The loop (Green) and NADH (purple) are shown. Images were created using Pymol (<http://www.pymol.org>) and Protein Data Bank (PDB) accession 5ZJD.

Fig.S2.

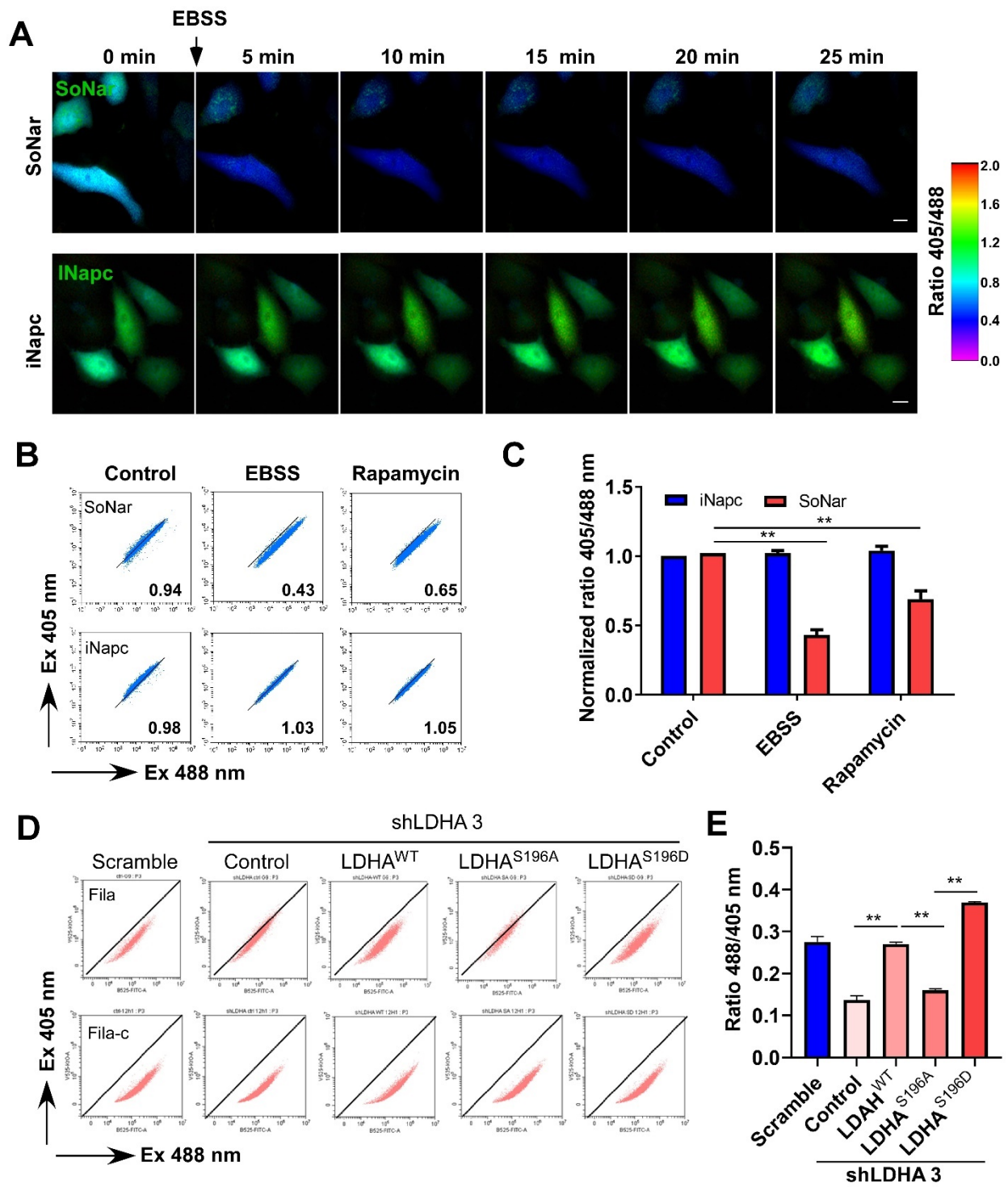


Fig.S2. ULK1 kinase activity regulates LDHA enzyme activity.

(A) Fluorescence images of SoNar and iNapc in HeLa cells treated with EBSS medium, scale bar, 10 μ m. iNapc was used as control sensor. (B) Representative flow-cytometric analyses of the SoNar and iNapc fluorescence upon EBSS medium and Rapamycin. iNapc was used as control sensor. (C) Quantification of (B). n=3. SoNar fluorescence ratio was corrected by iNapc. (D) Representative flow-cytometric analyses of the lactate sensor FiLa and FiLa-C in H1299 cells (control shRNA, LDHA KD/rescued by vector, LDHA^{WT}, LDHA^{S196A} and LDHA^{S196D}). (E) Quantification of (D). Data are shown as mean \pm SD; **p<0.01, n=3. FiLa fluorescence ratio was corrected by FiLa-C.

Fig.S3.

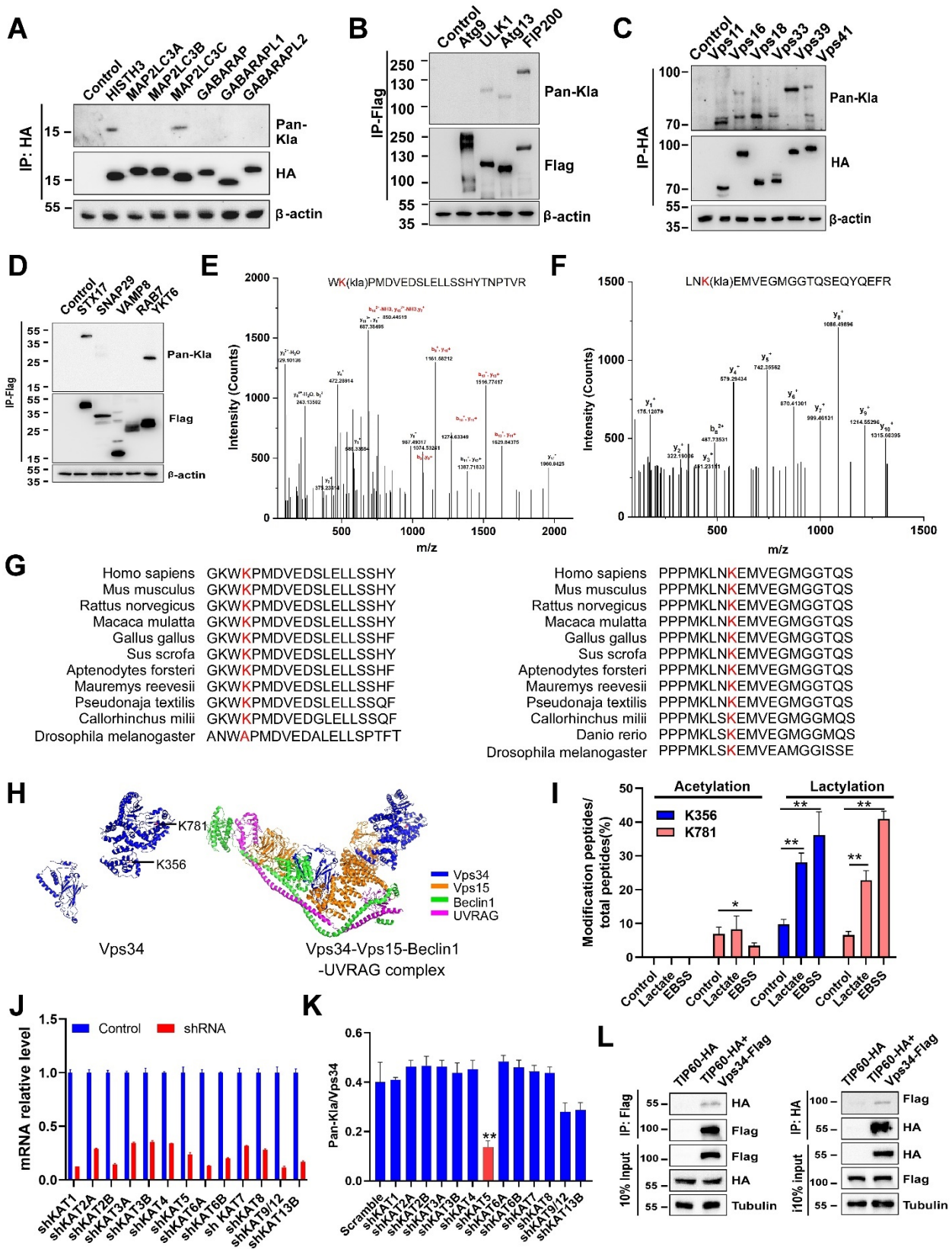


Fig.S3. TIP60 mediates Vps34 lactylation.

(A-D) Lactylation screening of autophagy core proteins in HEK293T cells. HA tagged or Flag-tagged autophagy core proteins were expressed individually in HEK293T cells and purified by Immunoprecipitation. Lactylation was analyzed by western blot with Pan-KIa antibody. (E) Identification of Vps34 lactylation at Lysine 356 by mass spectrometry. (F) Identification of Vps34 lactylation at Lysine 781 by mass spectrometry. (G) Alignment of sequences of Vps34 from various species. Red indicates the identified lactylation site of Vps34. (H) K356 and K781 sites in structure of Vps34 and Vps34-Vps15-Beclin1-UVRAG complex. Images were created using Pymol (<http://www.pymol.org>) and Protein Data Bank (PDB) accession 7BL1. (I) The acetylation and lactylation percentage of Vps34 K356 and K781 in normal medium, EBSS medium (3 h) and normal medium containing lactate (1 mM, 12 h) by mass spectrometry. Data are shown as mean \pm SD, ** $p < 0.01$, $n = 3$. (J) Relative mRNA expression level in acyltransferase knockdown HEK293T by fluorescence quantitative PCR. Data are shown as mean \pm SD, ** $p < 0.01$, $n = 3$. (K) Quantification of Figure 3F. Data are shown as mean \pm SD, ** $p < 0.01$, $n = 3$. (L) Vps34 interacts with TIP60. HA tagged TIP60 and Flag tagged Vps34 were co-expressed in HEK293T cells, Immunoprecipitation was performed and analyzed by western blot.

Fig.S4.

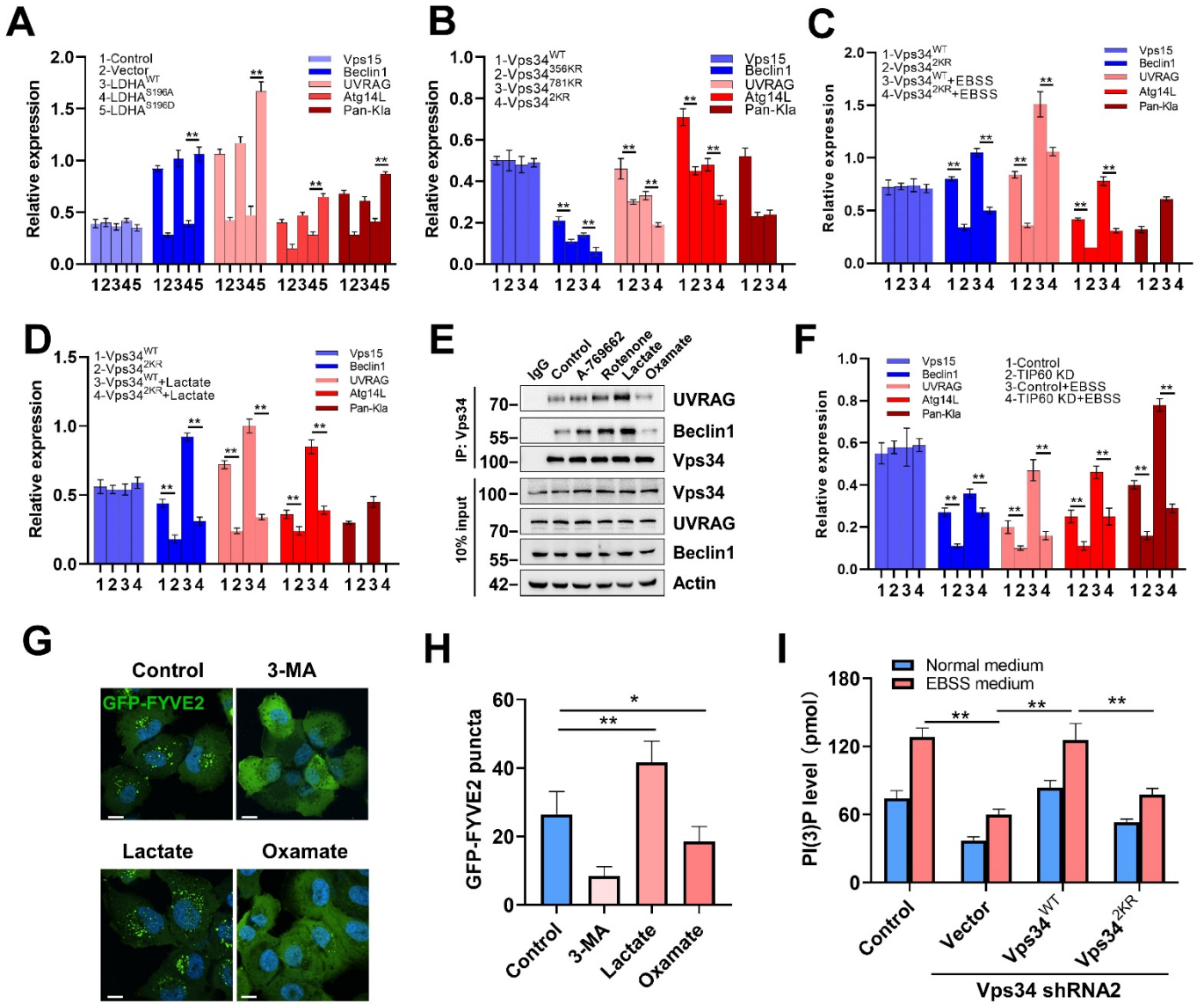


Fig.S4. Vps34 lactylation enhanced its lipid kinase activity by promoting interaction PI3KC3 subunits.

(A-D) Quantification of western blot in Figure 4A-4D. Data are shown as mean \pm SD, ** $p < 0.01$, $n=3$. (E) Interaction assay of Vps34 with Beclin1 and UVRAG in HEK293T cells that treated with A-769662 (100 nM), rotenone (10 nM), lactate (1 mM) and oxamate (10 mM). Immunoprecipitation was performed using Vps34 antibody and analyzed by western blot with anti-Beclin1 and UVRAG antibody. (F) Quantification of western blot in Figure 4E. Data are shown as mean \pm SD, ** $p < 0.01$, $n=3$. (G) Vps34 kinase activity assay by GFP-FYVE2. U2OS GFP-FYVE2 stable cell line was treated with 3-MA (2 mM), lactate (1 mM) and oxamate (10 mM) and analyzed by confocal microscopy. Scale bar, 10 μ m. (H) Quantification of GFP-FYVE2 puncta in (G). Data are shown as mean \pm SD; ** $p < 0.01$, $n=30$. (I) PI(3)P level determined by PI(3)P ELISA kit in HEK293T cells (control shRNA, Vps34 shRNA2/rescued by vector, Vps34^{WT} and Vps34^{2KR}). Data are shown as mean \pm SD; ** $p < 0.01$, $n=5$.

Fig.S5.

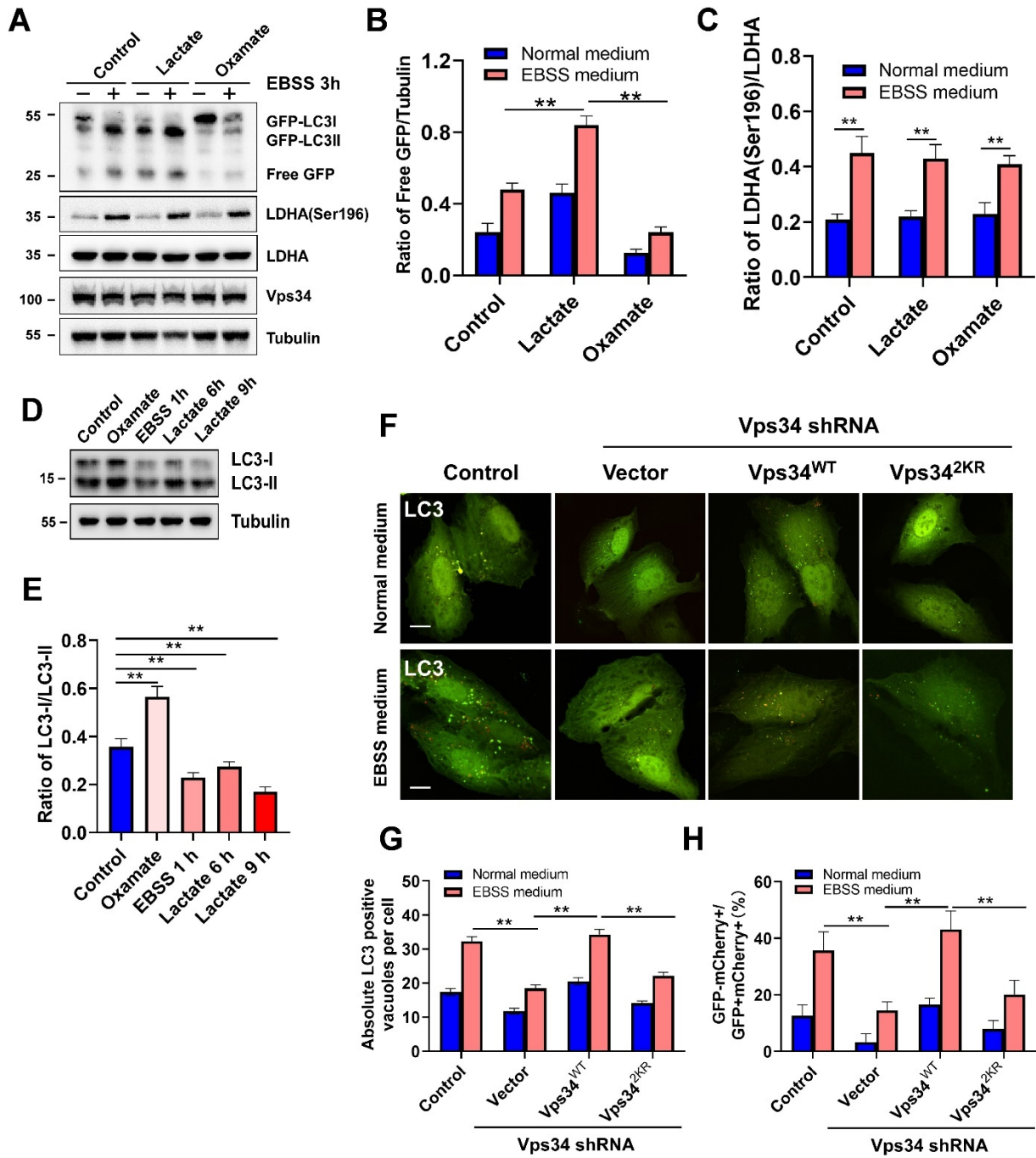


Fig.S5. Vps34 lactylation promotes autophagy

(A) GFP-LC3 cleavage assay. HEK293T cells were retreated with lactate (1 mM) and oxamate (10 mM) for 12 h under normal medium or EBSS medium for 2 h and analyzed by western blot with GFP antibody. (B) Quantification of free GFP/Tubulin in (A). Data are shown as mean \pm SD; ** $p < 0.01$, $n = 3$. (C) Quantification of LDHA (Ser196)/LDHA in (A). Data are shown as mean \pm SD; ** $p < 0.01$, $n = 3$. (D) Autophagy activity assay. HEK293T cells were treated with oxamate and lactate. Autophagy level was measured by LC3 turnover. (E) The ratio of LC3-I/LC3-II in (D). Data are shown as mean \pm SD; ** $p < 0.01$, $n = 3$. (F) Autophagosome maturation assay. mCherry-GFP-LC3 was transfected in U2OS cells (control shRNA, Vps34 KD, Vps34 KD/rescued by Vps34^{WT}, Vps34^{2KR}) under normal medium or EBSS medium for 2 h and analyzed by confocal microscopy. (G) Quantification of the relative GFP⁺mCherry⁺ LC3 puncta. which indicate autolysosomes in (E), Data are shown as mean \pm SD; ** $p < 0.01$, $n = 30$. (G) Quantification of the relative GFP⁺mCherry⁺ LC3 puncta. which indicate autolysosomes in (F), Data are shown as mean \pm SD; ** $p < 0.01$, $n = 30$. (H) The percentage of GFP⁺mCherry⁺ and GFP⁺ mCherry⁺ in (F), Data are shown as mean \pm SD; ** $p < 0.01$, $n = 30$.

Fig.S6.

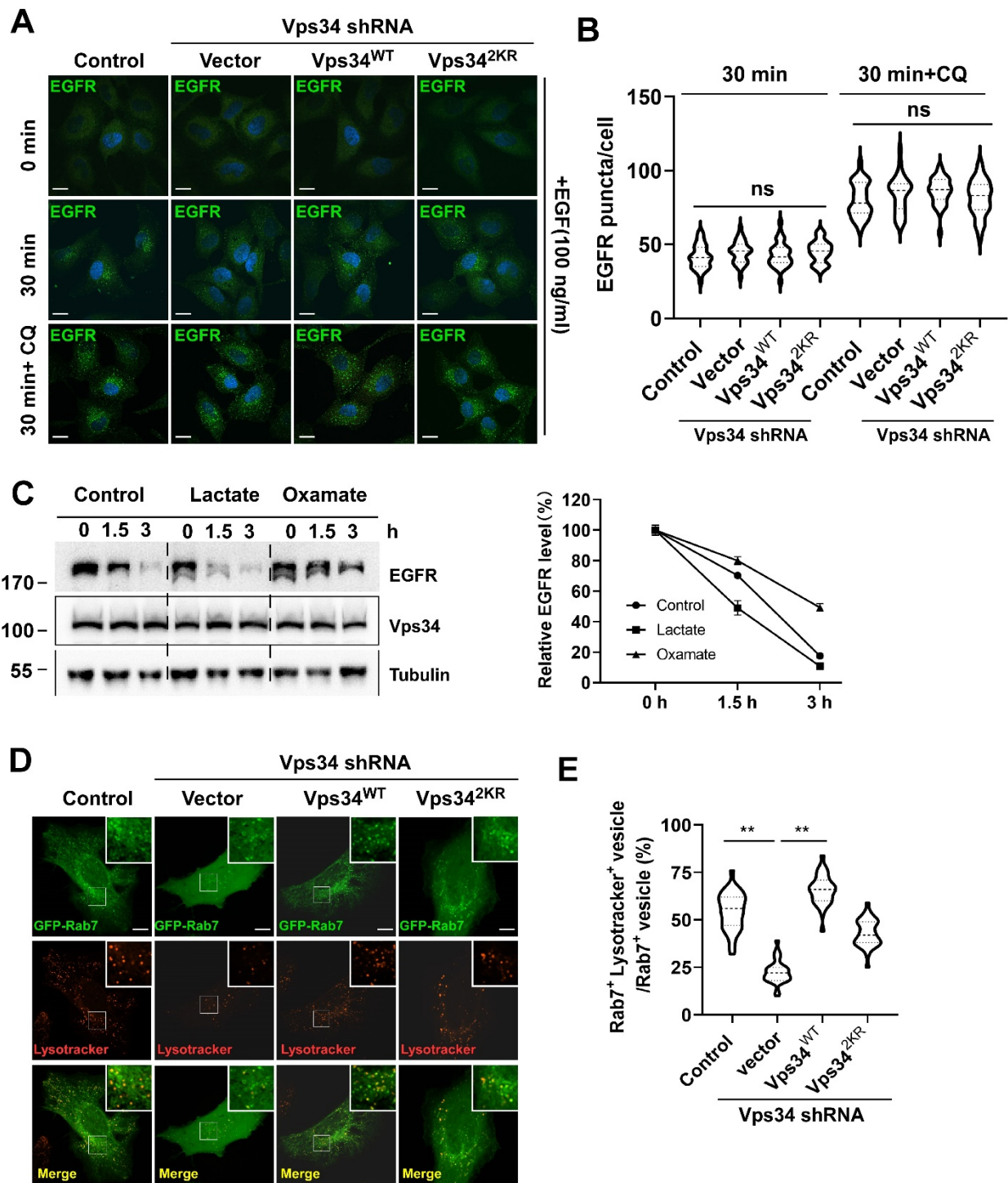


Fig.S6. Vps34 lactylation promotes endo-lysosomal trafficking

(A) Suppression of Vps34 expression does not impede internalization of the EGFR. HeLa cells (control shRNA, Vps34 KD, Vps34 KD/rescued by Vps34^{WT}, Vps34r^{2KR}) were stimulated with EGF (100 ng/ml) or EGF (100 ng/ml) and Chloroquine (CQ, 10 μ M) after overnight incubation with serum-free medium. Scale bar, 10 μ m. (B) Quantification assay of internalization of the EGFR in HeLa cells (control shRNA, Vps34 KD, Vps34 KD/rescued by Vps34^{WT}, Vps34r^{2KR}). Data are shown as mean \pm SD; n=30. (C) EGFR degradation assay. HEK293T cells were co-treated with lactate (1 mM) and oxamate (10 mM) with EGF (100 ng/mL) for 0 h, 1.5 h and 3 h. (D) EGFR levels were quantified by Image J software and normalized by percentage of 0 h EGFR level. Data are shown as mean \pm SD; **p<0.01, n=3. (E) Colocalization of GFP-Rab7 and lysotracker in U2OS cells (control shRNA, Vps34 KD/rescued by vector, Vps34^{WT} and Vps34^{2KR}). Colocalization of GFP-Rab7+ lysotracker+ vesicles were analyzed by confocal microscopy. Scale bar, 10 μ m. (F) Quantification of GFP-Rab7+ lysotracker+ vesicles per cell. Data are shown as mean \pm SD; **p<0.01, n = 30.

Fig.S7.

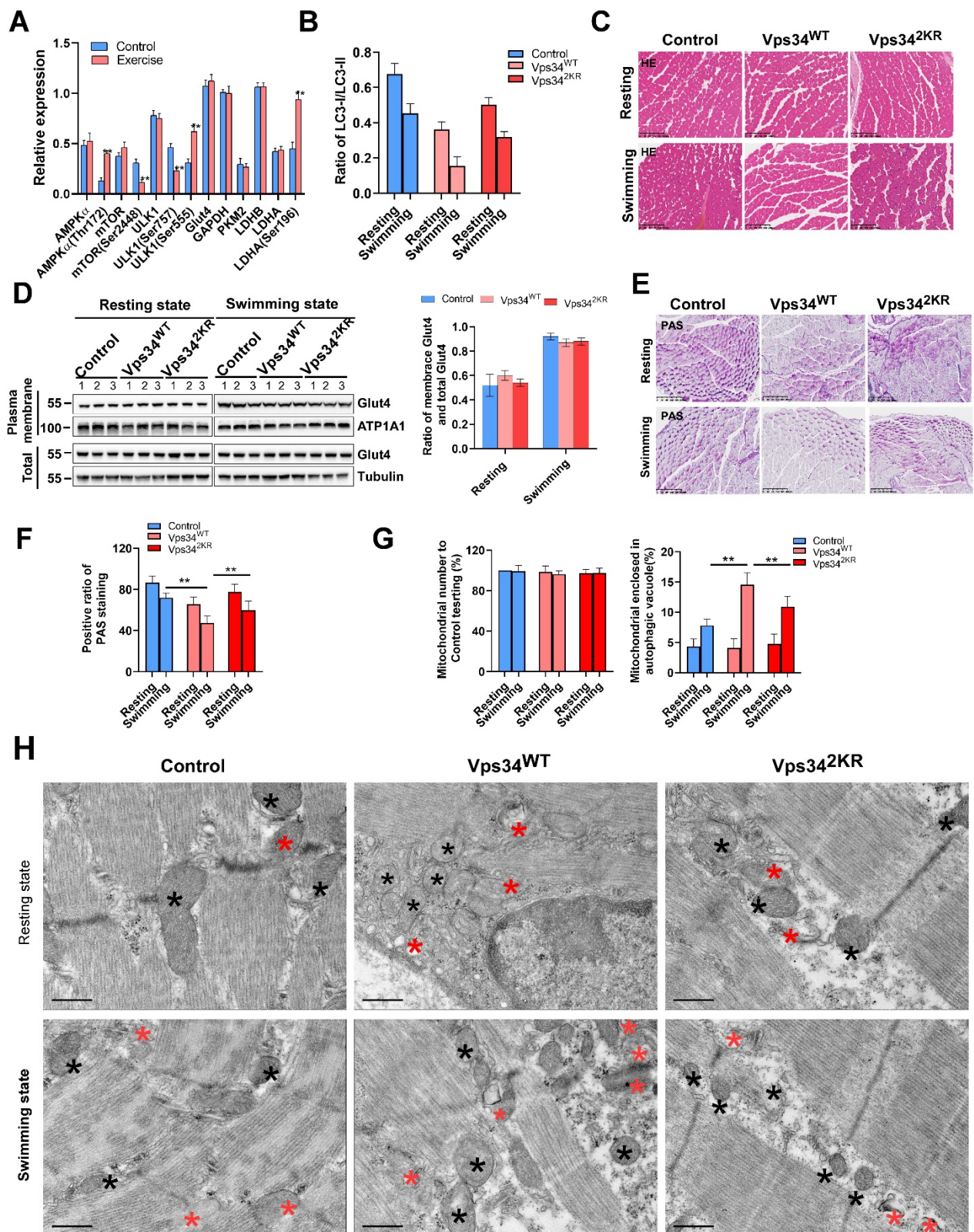


Figure S7. Vps34 lactylation is required for skeletal muscle homeostasis and cancer progress. Related to Figure 7

(A) Quantification assay of signaling pathway protein expression in mouse skeletal muscle of control group and swimming group by western blot in Figure 7A. Data are shown as mean \pm SD; ** $p < 0.01$, $n = 3$. (B) Quantification of LC3-I/LC3-II in Figure 7H. Data are shown as mean \pm SD; ** $p < 0.01$, $n = 3$. (C) H&E staining showing mice muscle histopathologic changes in control group, AAV-Vps34^{WT} group and AAV-Vps34^{2KR} group during resting state and swimming state. Scale bars, 200 μ m, $n = 5$. (D) Swimming promotes GLUT4 membrane distribution in mice muscle tissues of control group, AAV-Vps34^{WT} group and AAV-Vps34^{2KR} group by Western blot. Plasma Membrane Protein was Isolated by cell fractionation. Data are shown as mean \pm SD; ** $p < 0.01$, $n = 5$. (E) PAS staining showing glycogen level in mice muscle tissues of control group, AAV-Vps34^{WT} group, and AAV-Vps34^{2KR} group during resting state and swimming state. Scale bars, 50 μ m, $n = 5$. (F) Quantification analysis of PAS staining. Data are shown as mean \pm SD; ** $p < 0.01$, $n = 5$. (G) Quantification analysis of mitochondrial number and the percentage of mitochondria enclosed in an autophagic vacuole. Quantification data are shown as mean \pm SD; ** $p < 0.01$, $n = 10$. (G) Transmission electron microscopy showing the morphology of mitochondria and lysosome like structures in mice muscle tissues of control group, AAV-Vps34^{WT} group, and AAV-Vps34^{2KR} group during resting state and swimming state. Scale bars, 1 μ m. $n = 10$.

Table S1 Table S1 Lactylation peptides of Vps34 in vitro lactylation by mass spectrometry

Sequence	# PSMs	# Proteins	# Protein Groups	Protein Group Accessions	Modifications	ΔC_n	q-Value	PEP
SGPsDHDLPNAATR	1	3	1	Q8NEB9	S4(Phospho)	0.0000	0	0.01451
YAPSENGPnGISAEMDTYVK	9	6	1	Q8NEB9	N9(Deamidated)	0.0000	0	5.331E-10
YENFDDIKnGLEPTKK	4	3	1	Q8NEB9	N9(Deamidated)	0.0000	0	0.0000012
YENFDDIKnGLEPTK	4	3	1	Q8NEB9	N9(Deamidated)	0.0000	0	1.523E-07
YAPSENGPnGISAEMDTYVK	11	6	1	Q8NEB9	N9(Deamidated)	0.0000	0	2.241E-09
KYAPSEnGPnGISAEMDTYVK	1	6	1	Q8NEB9	N7(Deamidated)	0.0000	0	0.00003609
KYAPSEnGPNGISAEMDTYVK	9	6	1	Q8NEB9	N7(Deamidated)	0.0000	0	0.03263
YAPSEnGPnGISAEMDTYVK	1	6	1	Q8NEB9	N6(Deamidated)	0.0000	0	0.00002901
YAPSEnGPnGISAEMDTYVK	1	6	1	Q8NEB9	N6(Deamidated)	0.0000	0	7.177E-10
SGPSDHDLPnAATR	4	3	1	Q8NEB9	N11(Deamidated)	0.0000	0	0.00009001
KYAPSENGPnGISAEMDTYVK	4	6	1	Q8NEB9	N10(Deamidated)	0.0000	0	0.000002893
nGLEPTKK	1	3	1	Q8NEB9	N1(Deamidated)	0.0000	0	0.0116
nGLEPTK	2	3	1	Q8NEB9	N1(Deamidated)	0.0000	0	0.02933
DPKPLPPPmK	5	3	1	Q8NEB9	M9(Oxidation)	0.0000	0	0.000151
LNKEMVEGmGGTQSEQYQEFR	2	3	1	Q8NEB9	M9(Oxidation)	0.0000	0	0.001853
AVLEDPmLK	8	4	1	Q8NEB9	M7(Oxidation)	0.0000	0	0.003613
VPDPQmSmENLVESK	7	3	1	Q8NEB9	M6(Oxidation)	0.0000	0	5.176E-10
VPDPQmSMENLVESK	8	3	1	Q8NEB9	M6(Oxidation)	0.0000	0	3.457E-08
LNKEmVEGmGGTQSEQYQEFR	3	3	1	Q8NEB9	M5(Oxidation)	0.0000	0	0.0009105
SSNFmYlMVEFR	2	3	1	Q8NEB9	M5(Oxidation)	0.0000	0	0.000594
SSNFmYLMVEFR	2	3	1	Q8NEB9	M5(Oxidation)	0.0000	0	0.0004774
THEmYLNvmR	1	3	1	Q8NEB9	M4(Oxidation)	0.0000	0	0.004063
EIEmINSEKR	2	3	1	Q8NEB9	M4(Oxidation)	0.0000	0	0.00006621

EIEmINESEK	3	3	1	Q8NEB9	M4(Oxidation)	0.0000	0	0.0003825
THEmYLNVMR	5	3	1	Q8NEB9	M4(Oxidation)	0.0000	0	0.001136
WKPmDVEDSLELLSSHYTNPTVR	10	3	1	Q8NEB9	M4(Oxidation)	0.0000	0	1.55E-11
SALmPAQLFFK	6	4	1	Q8NEB9	M4(Oxidation)	0.0000	0	0.0003004
HGFmQFIQSVPAEVLDTGEGSIQNFFR	1	6	1	Q8NEB9	M4(Oxidation)	0.0000	0	0.0001724
EmVEGmGGTQSEQYQEFRK	1	3	1	Q8NEB9	M2(Oxidation)	0.0000	0	0.003474
EmVEGmGGTQSEQYQEFR	6	3	1	Q8NEB9	M2(Oxidation)	0.0000	0	2.148E-11
EmVEGMGGTQSEQYQEFR	7	3	1	Q8NEB9	M2(Oxidation)	0.0000	0	5.578E-11
HGDdLRQDQLILQIISLmDK	2	4	1	Q8NEB9	M18(Oxidation)	0.0000	0	0.0002385
KYAPSENGPNGISAEVmDTYVK	1	6	1	Q8NEB9	M17(Oxidation)	0.0000	0	0.00003675
QDQLILQIISLmDK	1	4	1	Q8NEB9	M12(Oxidation)	0.0000	0	0.000000412
LDLSDEEAVHYmQSLIDESVHALFAAVVEQIHK	2	3	1	Q8NEB9	M12(Oxidation)	0.0000	0	1.609E-11
LQALLGDNEKmNLSDELIPLEPQVK	1	3	1	Q8NEB9	M11(Oxidation)	0.0000	0.003	0.1538
TSSTLSEDQmSR	2	6	1	Q8NEB9	M10(Oxidation)	0.0000	0	0.000001516
mNLSDELIPLEPQVK	2	4	1	Q8NEB9	M1(Oxidation)	0.0000	0	6.635E-12
LNkEMVEGMGGTQSEQYQEFR	1	3	1	Q8NEB9	K3(Lactylation)	0.0000	0	0.000302
WkPMDVEDSLELLSSHYTNPTVR	3	3	1	Q8NEB9	K2(Lactylation)	0.0000	0	1.032E-09
GIIPETATLFKsALMPAQLFFK	1	4	1	Q8NEB9		0.0000	0.003	0.117
FSGLYQETcSDLYVTcQVFAEGKPLALPVR	4	4	1	Q8NEB9	C9(Carbamidomethyl)	0.0000	0	1.094E-09
FHYIYScDLdINVQLK	6	4	1	Q8NEB9	C7(Carbamidomethyl)	0.0000	0	0.0001072
KQcYTAFLHLR	5	3	1	Q8NEB9	C3(Carbamidomethyl)	0.0000	0	0.00001475
ScAGYcVITYILGVGDR	1	6	1	Q8NEB9	C2(Carbamidomethyl)	0.0000	0	2.46291E-13
QcYTAFLHLR	7	3	1	Q8NEB9	C2(Carbamidomethyl)	0.0000	0	0.0003119
TKEVPDGENLEQDLcTFLISR	3	3	1	Q8NEB9	C15(Carbamidomethyl)	0.0000	0	5.714E-08
EVPDGENLEQDLcTFLISR	4	3	1	Q8NEB9	C13(Carbamidomethyl)	0.0000	0	1.101E-09
cVnWDLQPQEAk	1	3	1	Q8NEB9	C1(Carbamidomethyl)	0.0000	0	0.0001585
cDDKEYGIVYYEK	6	3	1	Q8NEB9	C1(Carbamidomethyl)	0.0000	0	0.0002614
cVNWDLQPQEAk	5	3	1	Q8NEB9	C1(Carbamidomethyl)	0.0000	0	0.00001451

cDDKEYGIVYYEKDGEDESSPILTSFELVK	2	3	1	Q8NEB9	C1(Carbamidomethyl)	0.0000	0	7.541E-11
HGDDLK	1	19	1	Q8NEB9		0.0000	0	0.03664
NGLEPTKK	1	3	1	Q8NEB9		0.0000	0	0.03688
SGPSDHLKPNAATR	4	3	1	Q8NEB9		0.0000	0	1.411E-07
NGLEPTK	1	3	1	Q8NEB9		0.0000	0	0.05384
IGSLEGK	4	3	1	Q8NEB9		0.0000	0	0.04868
TSSTLSEDQMSR	7	6	1	Q8NEB9		0.0000	0	2.405E-07
DPKPLPPMK	12	3	1	Q8NEB9		0.0000	0	0.00008636
YYLTNQEK	11	3	1	Q8NEB9		0.0000	0	0.00509
EIEMINESEKR	6	3	1	Q8NEB9		0.0000	0	0.000002995
YFDLPR	15	6	1	Q8NEB9		0.0000	0	0.05416
YENFDDIK	6	3	1	Q8NEB9		0.0000	0	0.006574
EIEMINESEK	4	3	1	Q8NEB9		0.0000	0	0.00002276
LQALLGDNEK	16	3	1	Q8NEB9		0.0000	0	0.001277
FSQALLK	12	3	1	Q8NEB9		0.0000	0	0.07158
VWPNVEADGSEPTKTPGR	1	6	1	Q8NEB9		0.0000	0	0.004616
HLDNLLLTK	9	6	1	Q8NEB9		0.0000	0	0.0004425
TEDGGKYPVIFK	10	4	1	Q8NEB9		0.0000	0	2.193E-07
LPVKYFDLPR	3	6	1	Q8NEB9		0.0000	0	0.00006292
VWPNVEADGSEPTK	15	6	1	Q8NEB9		0.0000	0	7.511E-07
THEMYLNVMR	7	3	1	Q8NEB9		0.0000	0	0.00007128
YENFDDIKNGLEPTKK	2	3	1	Q8NEB9		0.0000	0	2.576E-08
EYGIVYYEK	2	3	1	Q8NEB9		0.0000	0	0.08536
VDWLDR	7	3	1	Q8NEB9		0.0000	0	0.04942
QALELLGK	4	3	1	Q8NEB9		0.0000	0	0.01052
AVLEDPMLK	4	4	1	Q8NEB9		0.0000	0	0.01162
YPVIFK	1	4	1	Q8NEB9		0.0000	0.003	0.1757
EMVEGMGGTQSEQYQEFR	3	3	1	Q8NEB9		0.0000	0	4.054E-11

SLLAQQTFVDR	19	3	1	Q8NEB9		0.0000	0	0.00002442
YENFDDIKNGLEPTK	2	3	1	Q8NEB9		0.0000	0	0.00001611
KYAPSENGPNGISAEVMDTYVK	2	6	1	Q8NEB9		0.0000	0	0.0001265
DQLNIIVSYPPTK	12	3	1	Q8NEB9		0.0000	0	6.669E-07
AVPVGGTTVSLFGK	14	6	1	Q8NEB9		0.0000	0	0.00003656
QLTYEEQDLVWK	6	3	1	Q8NEB9		0.0000	0	0.00004473
VPDPQMSMENLVESK	5	3	1	Q8NEB9		0.0000	0	7.791E-09
WKPMDEVDSLELLSHYTNPTVR	7	3	1	Q8NEB9		0.0000	0	4.515E-10
GIIPETATLFK	10	4	1	Q8NEB9		0.0000	0	0.0005927
DGDESSPILTSFELVK	3	3	1	Q8NEB9		0.0000	0	8.786E-09
SALMPAQLFFK	4	4	1	Q8NEB9		0.0000	0	0.00006161
NAQVALTIWDVYGPVK	4	6	1	Q8NEB9		0.0000	0	8.575E-11
WNWNEWLK	2	5	1	Q8NEB9		0.0000	0	0.0008799
LFHIDFGYILGR	2	3	1	Q8NEB9		0.0000	0	0.00005964
MNLSDELIPLEPQVK	3	4	1	Q8NEB9		0.0000	0	3.565E-10
SSNFMYLMVEFR	1	3	1	Q8NEB9		0.0000	0	0.002487
HGDDLRRDQLILQIISLMDK	3	4	1	Q8NEB9		0.0000	0	6.294E-07